

Effect of Irreversibility and Energy Harvesting on Entropy Generation Within A Microscale Heat Sink

Mahyar Pourghasemi^{a,*}

^a Department of Mechanical Engineering, University of New Mexico, USA
E-mail: *mpourghasemi@unm.edu

Received 25 March 2019, Revised 22 April 2019, Accepted April 23 January 2019

Abstract

In present work, the entropy generation minimization technique (EGM) is applied to study the performance of a microchannel heat sink combined with a new proposed parameter called irreversibility index and energy harvesting concept. Three different cases have been investigated using geometry of a microchannel heat sink selected from experimental works in the literature. The constraints considered in this study, are fixed channel height and maximum pressure drop. It has been observed that with fixed channel height constraint, while the aspect ratio changes from 1 to 10, the optimum operating condition fall in the range of Reynolds number equal to 2000 and aspect ratio of 2.25. Moreover, the extra constrain on maximum pressure drop imposes a limitation on applicable aspect ratio range. The maximum aspect ratio of the channel for stable flow field in this case cannot be higher than 5 imposed by criteria of laminar flow regime. The obtained optimum values are Reynolds number of 1850 and aspect ratio of 2. Using a combined new defined irreversibility index and Energy Harvesting Concept (EHC), it has been shown that the optimum design values for industrial applications are not necessary the ones obtained from EGM method and may shift to a new operating point based on the method considered for energy harvesting.

Keywords: Entropy generation; energy harvesting; irreversibility index; microchannel heat sink; design constraints.

1. Introduction

As the electronic devices get smaller, the heat dissipation rate gets larger and special treatments are needed to handle heat management. One of the solutions proposed by Tuckerman & Pease [1] is using microchannel heat sink. The advantages of microchannels are their smaller size, minimum coolant amount, high surface to volume ratio and low cost of maintenance and manufacturing. On the other hand, the most negative drawback of microchannel heat sinks that restricts their application is, the high pressure drop penalty paid for enhancing heat transfer rate.

Since the idea of microscale heat sink was proposed, several experimental and numerical investigations have been conducted to inspect fluid flow and heat transfer within such small scale devices. Early researchers attempted to answer the question whether flow field and heat transfer in microchannels follow the conventional fluid flow theories. Some early discrepancies reported around 1990s by Urbanek et al [2], Mala et al [3] and Pfahler et al. [4] which showed that the friction factor in micro tubes/channels are less or higher than ones for conventional laminar flow in macroscale tubes/channels. Researches correlated the observed differences to change in viscosity of fluid flow near micro-scale channel walls. El-Genk and Pourghasemi [5] conducted analytical and numerical simulations and showed that the apparent slip at the microchannel walls at small hydraulic diameter was the main cause of discrepancy between reported experimental data and conventional laminar values in macroscale channels. Later and most recent experimental and numerical investigations, have shown that for incompressible fluid flow within the microchannels and tubes, Navier-Stokes equation could be applied both for

single and multiphase flows with high level of confidence. Judy et al. [6] conducted experiments on friction factor within microtubes and microchannels at laminar flow regime with Reynolds number up to 2000. Authors concluded that the friction factors were similar to ones in macro scale tubes and channels within the uncertainty range of conducted experiments. Lee and Garimella [7] and Qu and Mudawar [8] conducted numerical and experimental studies on heat transfer within microchannels with different aspect ratios. Comparison between obtained experimental data and conducted numerical simulations showed that the Navier-Stokes equation could predict fairly well the fluid flow within micro-scale devices in single phase flow. Razi and Pourghasemi [9] also conducted two phase flow studies in micro-scale devices using direct numerical simulation approach. Comparison between obtained numerical results and experimental data illustrated that Navier-Stokes equation can predict two phase flow in micro-scale devices with fairly well accuracy.

Optimization of thermal device and heat exchangers is always an interesting topic in engineering field. Enhancing heat transfer rate while the pressure drop is fixed is the main goal of most optimization studies. Shortly, after microchannel heat sink idea was emerged, analytical and numerical studies have been performed to enhance the device performance through geometry optimization. Kim [10] compared three different models used to decrease the thermal resistance of microchannel heat sink within a fixed pressure drop. Garimella and Singhal [11] and Jang and Kim [12] analyzed experimentally the pumping requirements of microchannel heat sinks and optimized the size of the microchannels for minimum pumping requirements. Jang

and Kim [12] showed that the cooling performance of an optimized microchannel heat sink subject to an impinging jet is enhanced by about 21% compared to that of the optimized microchannel heat sink with parallel flow under the fixed-pumping-power condition.

Besides, the conventional method of enhancing thermal performance in a fixed pumping power, the second law of thermodynamics has been also applied to microchannel through entropy minimization technique. Cruz et al. [13] found that the best configuration was a copper aluminum heat sink with ammonia gas under considering three materials(silicon, aluminum, copper) and two working fluids(air, ammonia gas). Besides geometrical parameters, effect of apparent slip on entropy generation within microchannels is also studied analytically by Ebanez et al [14]. Results showed that the global entropy generation rate can be optimized using proper slip length at the channel walls. Different slip lengths can be achieved using manufactured hydrophobic surfaces for microchannels. Although, hydrophobic surfaces with apparent slip can lead to lower pumping power, high cost of manufacturing of microchannels with hydrophobic walls, has restricted the real world application of this kind of devices.

From the literature, it can be seen that most studies that utilized the second law of thermodynamics on optimization of micro-channel heat sinks geometry, tried to decrease the heat resistance while high pumping power and pressure drop were required. The high pumping power means high flow rate that force the microchannels to work in turbulent flow regime which is not practical. From the reported results available in the literature, even in a reasonable fixed pressure drop, the required optimum volume flow rate restricts the application of such devices in real life if liquids such as water are considered as working fluid. On the other hand, most previous studies investigated micro-scale heat sinks with gases and there is little work done on EGM optimization of heat sinks dealing with liquids such as water as working fluid.

Moreover, the analysis based on the second law of thermodynamics ignores the fact to tie the obtained optimum results to real world application of microchannel heat sinks. The optimum results obtained from EGM are not applicable in real life, unless an efficient energy harvesting process is introduced. Without combining the EGM results with efficient energy harvesting techniques, the obtained optimum geometries can be interpreted only as hypostasize ideal values without any significant industrial use.

In this study, the second law of thermodynamics is applied to a microchannel heat sink with water as working fluid and an analytical expression is derived for entropy generation rate. The entropy generation rate consists of two competing terms, entropy generation due to pressure drop and viscous friction as well as entropy generation due to heat transfer through finite temperature difference. In order to optimize the device geometry, the rate of entropy generation is considered as the objective function and then it is minimized to get the best solution based on the imposed constraints. Effort has been added to tie the results obtained from EGM method to engineering application through a new proposed irreversibility index and energy harvesting concept. With combined approach, EGM and Energy Harvesting concept, it has been observed that the optimum design values for heat sinks may shift to a new operating condition more suitable for real world industrial application. The main objective of the current study is therefore to bridge

between energy harvesting concept and entropy generation minimization technique to make the obtained optimal working conditions suitable for industrial application in micro-scale heat sinks. The irreversibility index is defined to correlate entropy generation minimization approach with energy harvesting concept.

2. Geometry and Physical Model

Figure 1, shows the heat sink geometry used in this study. Due to symmetry, only one channel has been analyzed and then the results are generalized to whole heat sink geometry by considering the total number of parallel channels in heat sink, "N". The top surface is assumed as perfectly insulated.

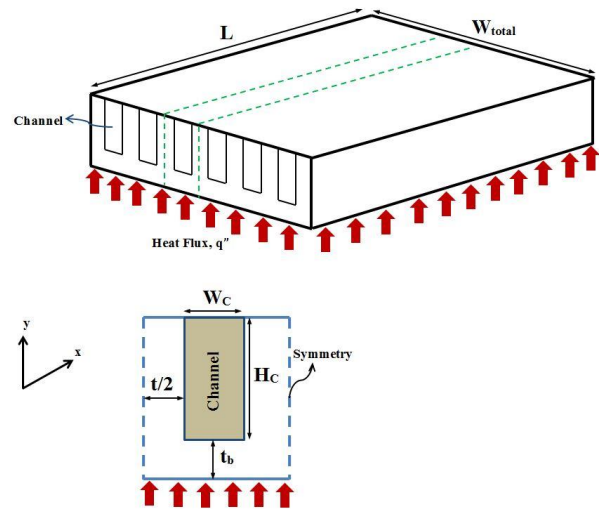


Figure 1. Schematic of the microchannel heat sink geometry used in this study.

The height of microchannel is H_c , the width is W_c , the lateral solid thickness is depicted by t . The thickness of base solid part is considered to be t_b . The total length of the channel is considered as L , and the total width of the heat sink is W_{total} .

From the geometrical constraint, it can be shown that the number of microchannels in the heat sink, N , is:

$$N = \frac{W_{total}}{W_c + t} \quad (1)$$

The first and the second law of thermodynamics as well as fundamental thermodynamic relation, for a differential element of length "dx" along the channel axis, leads to:

$$q''(W_c + t) = \dot{m} \frac{dh}{dx} \quad (2)$$

$$-\dot{m}ds + \dot{S}_{gen} + \frac{q''(W_c + t)dx}{T_b} = 0 \Rightarrow \frac{d\dot{S}_{gen}}{dx} = \dot{m} \frac{ds}{dx} - \frac{q''(W_c + t)}{T_b} \quad (3)$$

$$dh = T_f ds + \frac{1}{\rho} dP \Rightarrow \frac{dh}{dx} = T_f \frac{ds}{dx} + \frac{1}{\rho} \frac{dP}{dx} \quad (4)$$

where, q'' is heat flux, \dot{m} is the mass flow rate for a single channel ($\frac{\dot{m}_{total}}{N}$), P is the pressure, ρ is the fluid bulk density, "h" is the enthalpy of the working fluid (water in this study),

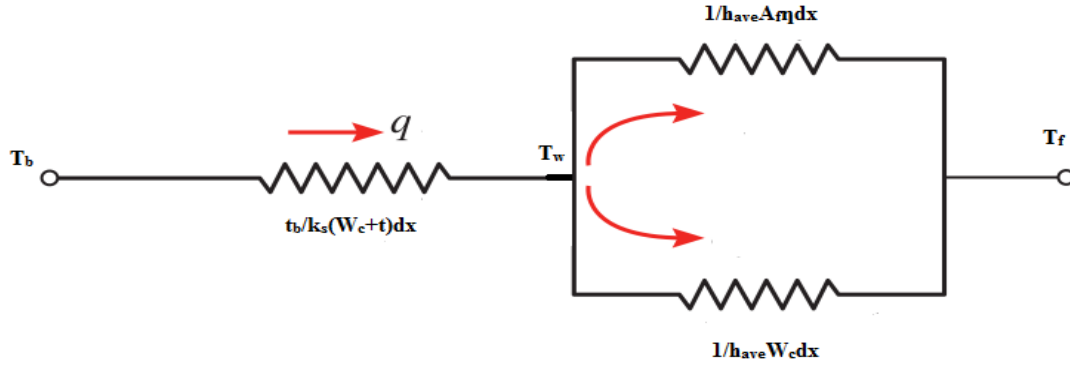


Figure 2. Equivalent thermal resistance network for a differential element of length “dx” along the heat sink length investigated in this study (see Figure 1)

T_b is the temperature of the base solid changing with x along the channel. T_f , is the bulk temperature of the fluid at any location, x .

Combining Eqs. (2), (3) and (4), the following relation between entropy generation, heat flux and pressure drop is obtained for the heat sink.

$$\dot{S}'_{gen} = \frac{d\dot{S}_{gen}}{dx} = q'' * (W_c + t) \frac{T_b - T_f}{T_b T_f} - \frac{\dot{m}}{\rho T_f} \frac{dP}{dx} \quad (5)$$

The side walls of the channel can be treated as thin fins with adiabatic tip. It is a reasonable approximation as the thickness of side walls are much smaller than the channel length, ($t \ll L$ in Figure 1) and they behave like fins. Figure 2 also depicts the equivalent thermal resistance network for the differential element of length “dx” along the heat sink length. Eqs. (6) and (7) present the equivalent thermal resistance and heat flux transferred to working fluid.

$$\begin{aligned} R_{base} &= \frac{t_b}{k_s (W_c + t) dx} \\ R_{bottom_wall_conv} &= \frac{1}{h_{ave} (W_c) dx} \\ R_{side_walls_conv} &= \frac{1}{h_{ave} (2H_c \eta_f) dx} \\ R_{total} dx &= R_{base} + \left(\frac{1}{R_{bottom_wall_conv}} + \frac{1}{R_{side_walls_conv}} \right)^{-1} \\ &= \frac{1}{k_s (W_c + t)} + \frac{1}{h_{ave} (W_c + 2H_c \eta_f)} \end{aligned} \quad (6)$$

$$q'' (W_c + t) = \frac{T_b - T_f}{R_{total}} = \frac{T_b - T_f}{\frac{1}{k_s (W_c + t)} + \frac{1}{h_{ave} (W_c + 2H_c \eta_f)}} \quad (7)$$

where, h_{ave} , is the convective heat coefficient at any location x along the channel. η_f is the fin efficiency (side walls of the channel that are considered as thin fins). k_s , is the thermal conductivity of heat sink base material that considered to be copper in this study.

Substituting Eq. (7) in (5), the correlation for entropy generation rate is changed as Eq. (8).

$$\dot{S}'_{gen} = \frac{d\dot{S}_{gen}}{dx} = \frac{q'' * (W_c + t)^2 R_{total}}{[q'' R_{total} (W_c + t) + T_f] T_f} - \frac{\dot{m}}{\rho T_f} \frac{dP}{dx} \quad (8)$$

Assuming uniform heat flux over the heat sink length and using the Darcy friction factor, Temperature of the fluid at any location x as well as pressure drop are obtained, Eq. (9):

$$\begin{aligned} T_f(x) &= T_{f,in} + \frac{q'' * (W_c + t)}{\dot{m} c_p} x \\ \frac{dP}{dx} &= f \frac{1}{2D_h} \rho V^2 \Rightarrow \dot{m} = \rho A_c V \Rightarrow \frac{dP}{dx} = \frac{f}{D_h} \frac{\dot{m}^2}{2\rho A_c^2} \end{aligned} \quad (9)$$

The final form of entropy generation rate for the differential element of length dx is obtained by combining Eqs. (9) and (8).

$$\begin{aligned} \dot{S}'_{gen} &= \frac{d\dot{S}_{gen}}{dx} = \frac{q'' * (W_c + t)^2 R_{total}}{[q'' R_{total} (W_c + t) + T_f] T_f} - \frac{f}{D_h} \frac{\dot{m}^3}{2\rho^2 A_c^2 T_f} \\ T_f(x) &= T_{f,in} + \frac{q'' * (W_c + t)}{\dot{m} c_p} x \end{aligned} \quad (10)$$

Total entropy generation due to friction and heat transfer for whole microscale heat sink, is obtained by taking the integral from both sides in Eq. (10) microchannel.

$$\dot{S}_{gen} = \int_0^L \dot{S}'_{gen} dx \quad (11)$$

In order to solve this integral and calculate the entropy generation rate, the following correlations have been used in this study to evaluate Nusselt number and friction factor in microscale heat sinks.

Friction factor [16]:

$$f Re_{ave,0-L_c} = \sqrt{\left[\frac{3.2}{\left(\frac{L_c}{D_h} Re \right)^{0.57}} \right]^2 + (f Re)_{fd}^2} \quad (12)$$

$$(f Re)_{fd} = 96 \left(1 - 1.3553\alpha + 1.9467\alpha^2 - 1.7012\alpha^3 + 0.9564\alpha^4 - 0.2537\alpha^5 \right)$$

where, α is the channel aspect ratio, $\alpha = \frac{H_c}{W_c}$.

Nusselt Number [7, 15]:

$$Nu_4 = \frac{1}{C_1(z^*)^{C_2} + C_3} + C_4 \quad 1 < \alpha < 10, x^* < x_{th}^*$$

Where

$$C_1 = -2.757 * 10^{-3} \alpha^3 + 3.274 * 10^{-2} \alpha^2 + 7.464 * 10^{-5} \alpha + 4.476$$

$$C_2 = 6.391 * 10^{-1}$$

$$C_3 = 1.604 * 10^{-4} \alpha^2 - 2.622 * 10^{-3} \alpha + 2.568 * 10^{-2}$$

$$C_4 = 7.301 - \frac{13.11}{\alpha} + \frac{15.19}{\alpha^2} - \frac{6.094}{\alpha^3}$$

non-dimensional thermal longitudinal position

$$x^* = \frac{x}{(D_h \text{RePr})}$$

non-dimensional Thermal developing length

$$x_{th}^* = -1.275 * 10^{-6} \alpha^6 + 4.709 * 10^{-5} \alpha^5 - 6.902 * 10^{-4} \alpha^4 + 5.014 * 10^{-3} \alpha^3 - 1.769 * 10^{-2} \alpha^2 + 1.845 * 10^{-2} \alpha + 0.05691$$

The average Nusselt number for whole channel is evaluated using Eq (13).

$$Nu_{ave} = Nu_4 * \left(\frac{Nu_{3d}}{Nu_{4d}} \right) \quad (13)$$

$$Nu_{3d} = 8.235 \left(1 - 1.883\alpha + 3.767\alpha^2 - 5.814\alpha^3 + 5.361\alpha^4 - 2\alpha^5 \right)$$

$$Nu_{4d} = 8.235 \left(1 - 2.0421\alpha + 3.0853\alpha^2 - 2.4765\alpha^3 + 1.0578\alpha^4 - 0.1861\alpha^5 \right)$$

Figures 3 and 4 illustrate the comparison between correlations (12)-(13) and some experimental data form literature. It can be seen that the used correlations in this study is accurate and follow the physical trend by a maximum deviation of 10 percent.

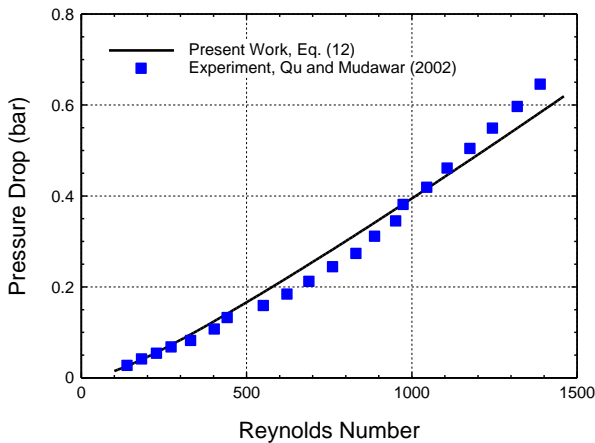


Figure 3. Comparison between experimental data [8] and Eq. (12) for pressure drop.

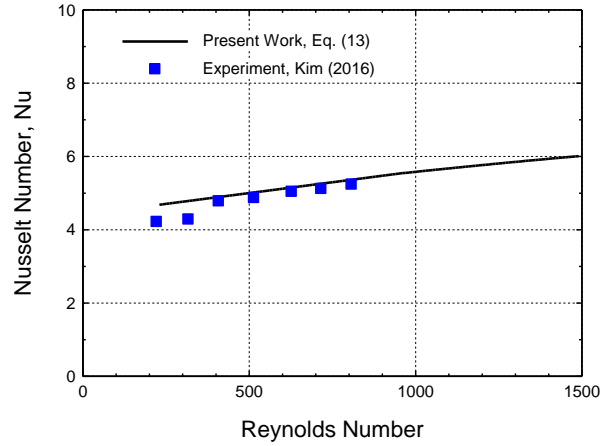


Figure 4. Comparison between experimental data [17] and Eq. (13) for Nusselt number.

3. Optimization Case Studies

The main assumption for all case studies in this work, are:

- a: Water as working fluid, b: Rectangular cross section for microchannels in heat sink with aspect ratio range of 1 to 10. c: Laminar flow regime with maximum Reynolds number of 2000. d: Incompressible fluid flow with temperature dependent properties of $\rho(T_f), \mu(T_f), K(T_f)$.
- e: Insulated top surface for heat sink (see Figure 1) with no heat loss with surrounding environment

3.1 Case I

To apply the EGM technique, we first considered the geometry of microchannel heat sink used in the experimental work by Qu and Mudawar [8]. They used a rectangular cross-sectional micro scale heat sink with aspect ratio of 3 and Reynolds number range of 130-1700. The channels were made of copper and deionized water was used as the working fluid. Table 1 summarizes the geometry of micro heat sink used in experimental study by Qu and Mudawar [8].

Table 1. The channel geometry, Reynolds number range and heat flux used in Case I, [8].

$H_c(\mu m)$	$W_c(\mu m)$	N(#Channels)	Re	$q''(W/cm^2)$
713	231	21	130-1700	100

The entropy generation rate is calculated by taking the integral in Eq. (11) simultaneously considering Eqs. (12) and (13). The aim is to find the optimum mass flow rate and corresponding Reynolds number in laminar flow regime that minimizes the entropy generation rate in heat sink. This will be the best operating point for the micro-channel heat sink used in the experiment based on the second law approach (EGM).

Figure 5, illustrates the total entropy generation rate as a function of Reynolds number for heat sink in this section. It can be seen that the minimum entropy generation rate occurs at Reynolds number of 1250. This point is the best operating condition for the device according to second law of thermodynamics (EGM technique).

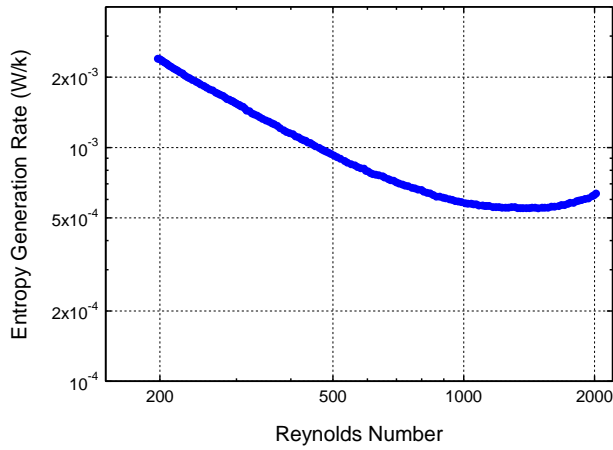


Figure 5. Entropy generation rate as a function of Reynolds number for case I.

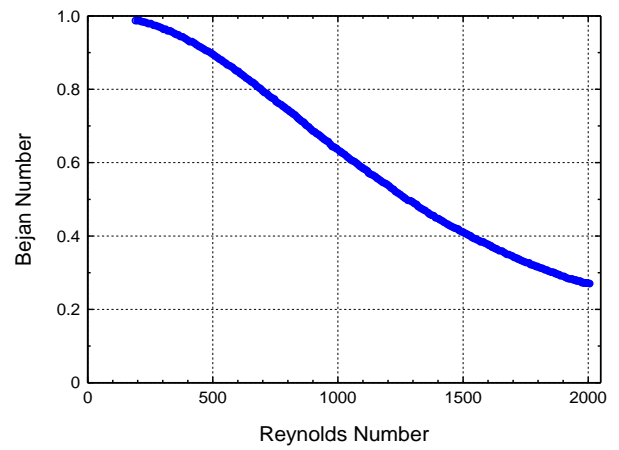


Figure 6. Bejan number as a function of Reynolds number for case I.

In order to investigate further the obtained results, the definition of Bejan number as well as a new parameter defined by author, "Irreversibility index", are considered in Eq. (14).

$$Be = \frac{S_{gen}(\text{Due to heat transfer})}{S_{gen}(\text{Total entropy generation})}$$

$$\psi = \text{Irreversibility index} = \frac{\text{total work}}{\text{Total heat removed}}$$

$$= \frac{\text{Pumping power} + \text{lost work}}{\text{Total heat applied from bottom to heat sink}} \quad (14)$$

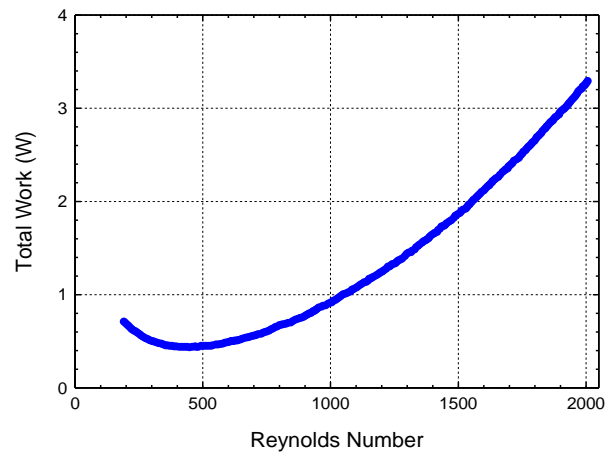


Figure 7. Total work defined in Eq. (14) as a function of Reynolds number.

$$\text{Pumping power} = \Delta P * \dot{m} / \rho$$

$$\text{Lost work} = T_{amb} * \dot{S}_{gen}$$

The Irreversibility index, ψ , is an indicator of total work which measures the work done by pump to overcome the friction force plus the energy that can be harvested as useful work.

Figures 6 to 8, present the Bejan number, total work and irreversibility index as a function of Reynolds number for case I. It can be noticed that, Bejan number is high at low Reynolds number range and by increasing the Reynolds number, it gets smaller. At low Reynolds number, The entropy generation within the heat sink is dominated by heat transfer mechanism, but at Reynolds number larger than 1250, the irreversibility due to fluid friction becomes more significant than the entropy generation due to heat transfer. From Figures 5 and 6, it can be noticed that the best operating point obtained from second law approach (EGM) is almost coincides with the transition point (Bejan number=0.5), where entropy generation rate changes from heat dominated to pressure dominated.

Based on the second law of themodynamics, the obtained value for Reynolds number from EGM technique in this section, corresponds to the best thermal design point (optimum Reynolds number or mass flow rate) that minimize entropy generation rate in heat sink for removing constant amount of heat. To further investigate this conclusion, author defined ψ , irreversibility index in Eq. (14).

The entropy generation times ambient temperature, gives the total work that have been lost during the process of removing heat in heat sink. The EGM technique and second law of thermodynamics inherently rely on Energy harvesting concept. The obtained Reynolds number from EGM technique in this section, $Re \sim 1250$, is the best operating condition if efficient energy harvesting techniques are designed to convert the lost work to useful power and compensate some portion of required pumping power. In the absence of such efficient energy harvesting techniques in current academic and industrial environment, the author suggests that it is more practical to consider combination of lost work and pumping power as objective function to obtain the optimum design point. It can be interpreted as a bridge to fill the gap between ideal optimum condition obtained from EGM technique and optimum thermal design point for real industrial application.

For example, in ideal case with EGM technique it can be assumed that some energy can be harvested using an ideal thermoelectric device working between heat sink bottom wall and bulk fluid temperatures. Using this concept, some energy can be harvested and used to run the pump and therefore reduce the total pumping power. The optimum operating point therefore would be one obtained from EGM i.e. $Re = 1250$. However, in the microchannel heat sink in this case, no energy has been harvested; therefore, the irreversibility index has been proposed to address the total

penalty paid to remove fixed amount of heat through heat sink. The best operating point based on irreversibility index therefore, is the condition that has lowest total work or correspondingly lowest irreversibility index, see Figure 8.

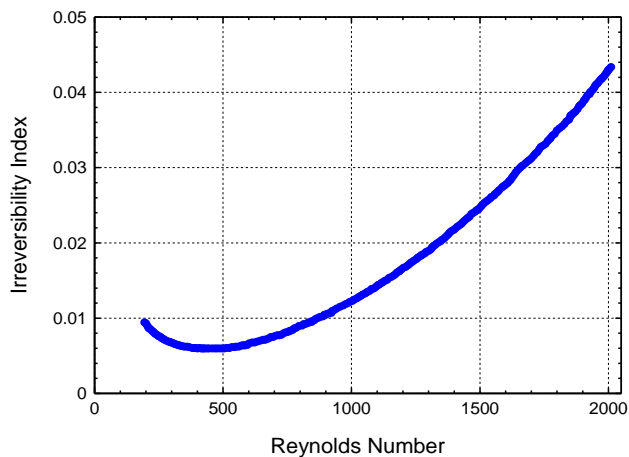


Figure 8. Irreversibility index defined in Eq. (14) as a function of Reynolds number.

As it can be seen from Figure 8, the optimum design point shifts from Reynolds number of 1250 to 450 if total lost work is considered as objective function and no energy is harvested.

It can be noticed that the obtained results from EGM technique (Rey ~ 1250) does not necessarily coincide with the optimum values from irreversibility concept. In a nutshell, the energy harvesting concept and defined irreversibility index indicate that the optimum design values emerged from EGM technique is reliable if there are efficient methods available for energy harvesting. Otherwise, the optimum values can be interpreted as the ideal optimum parameters that cannot be used in industrial environment. Without an efficient energy harvesting method, the author suggests using the irreversibility index as objective function, since it minimizes the total work in the process, (pumping power and lost work).

3.2 Case 2: Optimization of channel Aspect Ratio

3.2.1 Case A, Fixed Channel Height

In the section 3.1 (Case I), the entropy generation rate for heat sink used by Qu and Mudawar [8] in deferent Reynolds numbers has been investigated and optimum working condition has been obtained using EGM technique.

In this section, the effect of channel geometry on its performance is studied. For this purpose, first, the height of channel is kept constant and the aspect ratio changes from 1.25 to 9.75. The main goal is to determine in what aspect ratio, the minimum entropy generation rate occurs and then at that optimum aspect ratio, the optimum mass flow rate and corresponding Reynolds number is evaluated by EGM technique. The minimum entropy generation rate within the channels with different aspect ratio and constant height is presented in Figure 9. It can be seen that the aspect ratio of 2.25 is the best design point with constraint of constant channel height and objective function of lowest entropy generation.

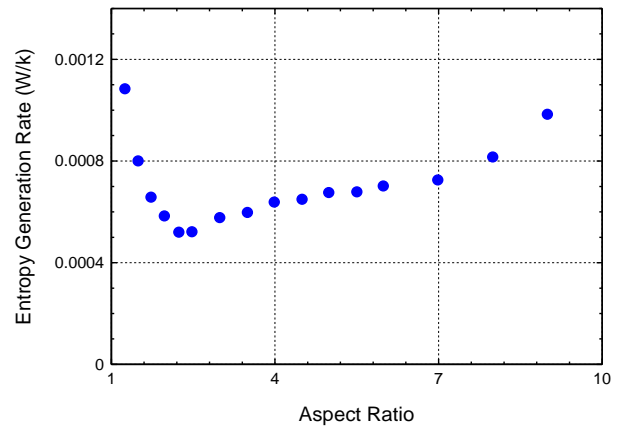


Figure 9. Entropy generation rate as a function of channel aspect ratio, fixed channel height constraint.

In order to further investigate the channel with optimum aspect ratio of 2.25, the entropy generation in different Reynolds numbers has been calculated and shown in Figure 10. Figure 10 illustrates that the optimum Reynolds number in a channel with optimum aspect ratio of 2.25 is 2000 if the flow regime considered laminar. It is consistent with the result in Figure 11. As it can be seen, the Bejan number is still higher than 0.5 which means that for all Reynolds number in this aspect ratio the entropy generation due to heat transfer is dominant and therefore increasing the Reynolds number leads to transferring heat in a lower temperature difference. It means that the irreversibility reduces in the heat sink.

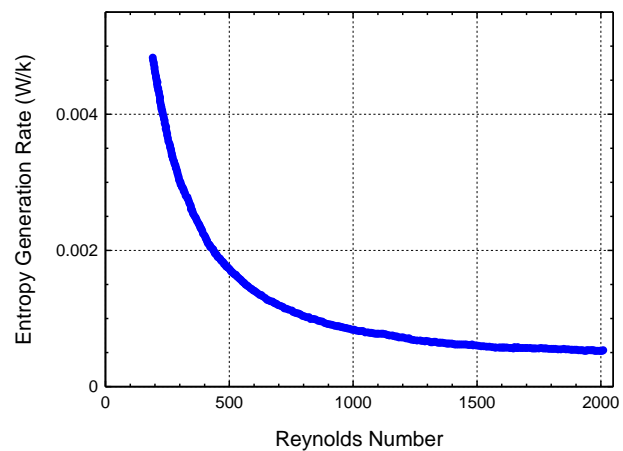


Figure 10. Entropy generation rate as a function of Reynolds number for channel with optimum aspect ratio of 2.25.

In order to see if the optimum working point obtained from EGM method coincides with optimum design point based on the irreversibility index, the lost work and irreversibility index have been shown in Figures 12 and 13, respectively. It can be seen that the best operating condition based on the irreversibility index is around Reynolds number of 700. It indicates that with no energy harvesting the optimum design point fall around Reynolds number of 700 instead of 2000. This fact results in a large pumping power difference as mass flow rate will decrease significantly within heat sink.

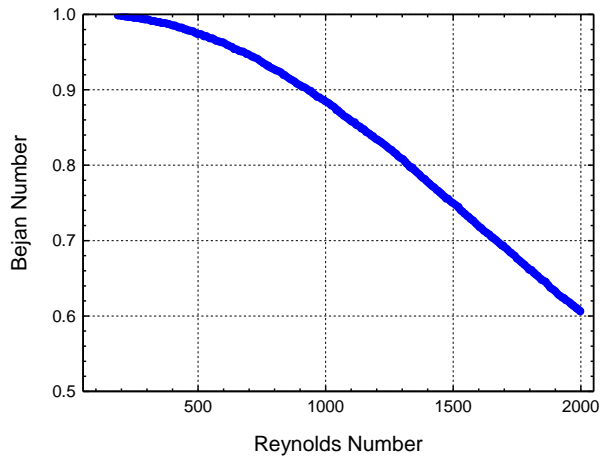


Figure 11. Bejan number as a function of Reynolds number for case with optimum aspect ratio of 2.25.

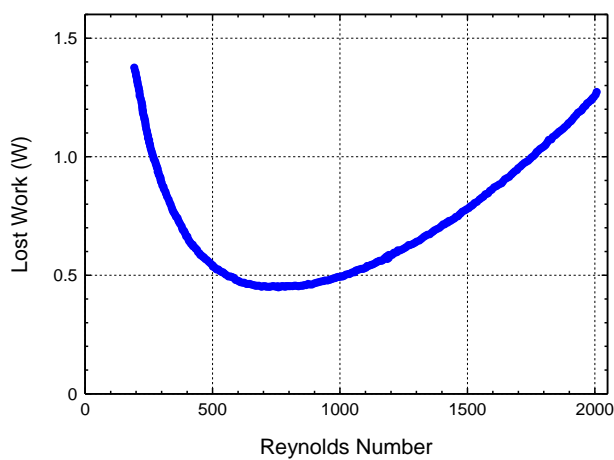


Figure 12. Total work defined in Eq. (14) as a function of Reynolds number for case with optimum aspect ratio of 2.25.

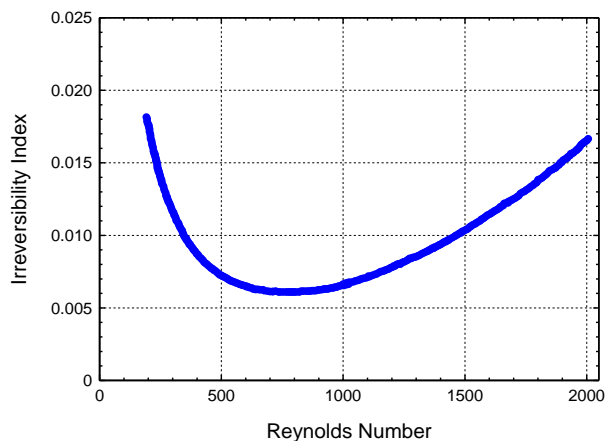


Figure 13. Irreversibility index defined in Eq. (14) as a function of Reynolds number for case with optimum aspect ratio of 2.25.

3.2.2) Case B, Maximum pressure drop constraint at Fixed Channel Height

In industrial environment and real application of microchannel heat sinks, pressure drop is a main constraint limiting the performance of micro scale heat sinks. The overall pressure drop is high as the ratio of surface area to

volume is very high in microscale devices. Therefore, it is assumed that the maximum pressure drop should not exceed 0.5 bar in this section. This constraint is applied to instigate the optimum aspect ratio and working condition for microscale heat sink presented in Figure 1.

From Figure 14, it can be seen that if Reynolds number is allowed to increase up to 2000 and flow field is considered laminar, the pressure drop constraint of 0.5 bar, reduces the highest practical channel aspect ratio to 5 instead of 10. For higher aspect ratios, the pressure drop within heat sink exceeds the threshold of 0.5 bar before optimum Reynolds number is reached. It can be inferred that for aspect ratio higher than 5, the maximum pumping power associated with maximum pressure drop threshold (0.5 bar) is not sufficient enough to keep stable flow field within microchannel heat sink before minimum entropy generation rate appears. It is also clear that by applying the extra constraint on pressure drop, the optimum aspect ratio shifts from 2.25 to 2.0.

Entropy generation and Bejan number within a channel with aspect ratio of 2 and maximum pressure drop constraint of 0.5 bar, have been presented in Figures 14 and 15. It can be seen that the extra constraint on pressure drop changes the optimum working condition from Reynolds number of 2000 to almost 1850.

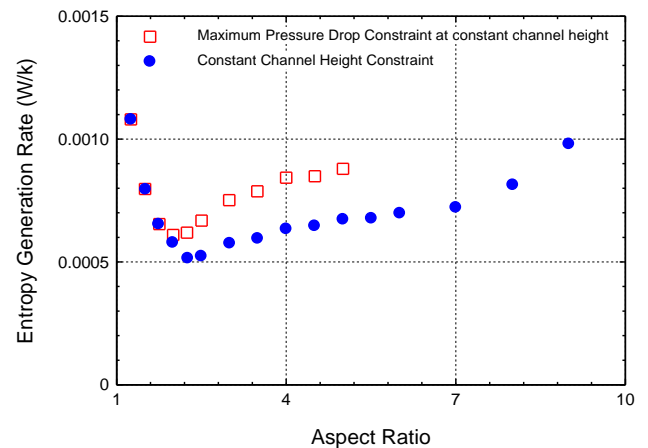


Figure 14. Effect of aspect ratio on entropy generation rate at constant channel height with and without maximum pressure drop constraint.

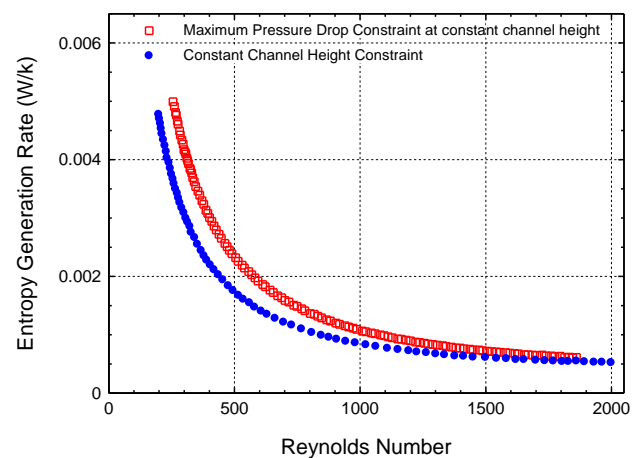


Figure 15. Entropy generation rate as a function of Reynolds number for optimum aspect ratio at constant channel height with and without maximum pressure drop constraint.

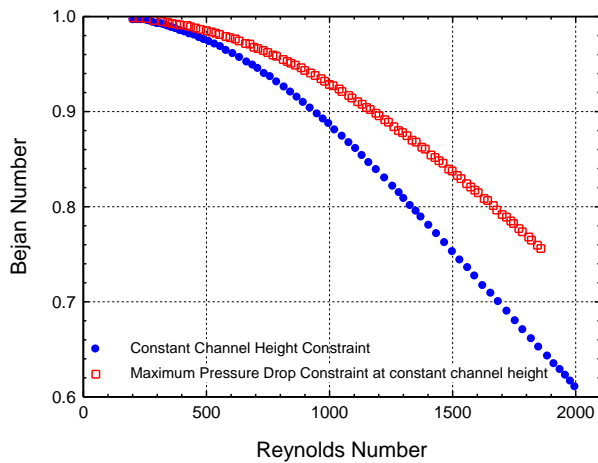


Figure 16. Bejan number as a function of Reynolds number for optimum aspect ratio at constant channel height with and without maximum pressure drop constraint.

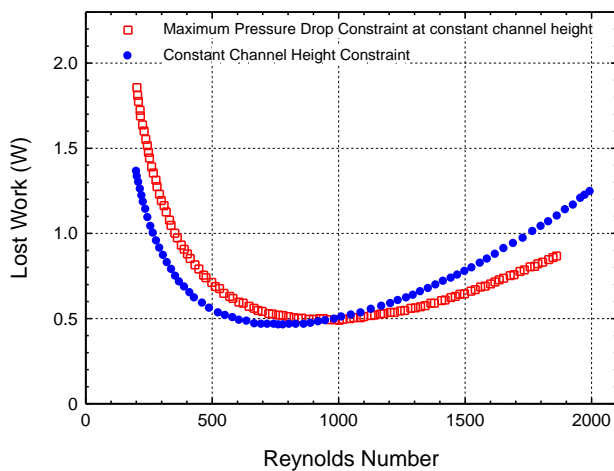


Figure 17. Total work defined in Eq. (14) as a function of Reynolds number for optimum aspect ratio at constant channel height with and without maximum pressure drop constraint.

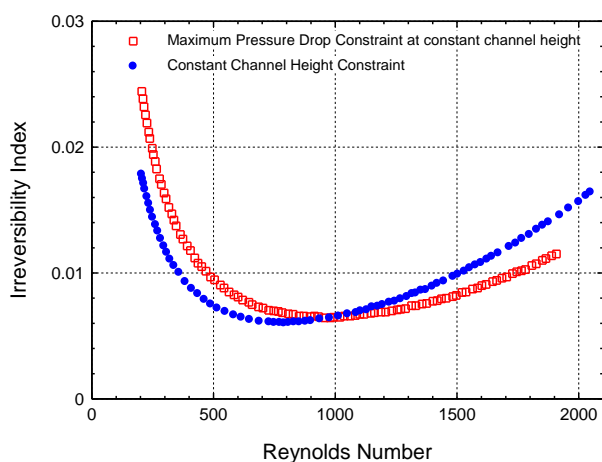


Figure 18. Irreversibility index defined in Eq. (14) as a function of Reynolds number for optimum aspect ratio at constant channel height with and without maximum pressure drop constraint.

The lost work and irreversibility index have been shown in Figures 17 and 18 as well. It can be inferred from the figures that the best design point from irreversibility index approach shifts from Reynolds 700 to Reynolds 900 due to the extra constrain of maximum pressure drop.

Conclusion

The performance of a microchannel heat sink has been investigated using EGM approach. First, one experimental set-up used by QU and Mudawar [8] investigated to obtain the optimum working condition for mass flow rate without any constraints. The results show that the optimum Reynolds number is around 1250 proposed by EGM technique relying on second law of thermodynamics. Moreover, in the second case, the constraint was applied to channel height (Fixed channel height of 713 micrometers) while the aspect ratio changes from 1 to 10. In this case the optimum aspect ratio and corresponding Reynolds number have been determined as 2.25 and 2000, respectively.

In the Third case, an extra constrain is applied to maximum pressure drop along the channel while the channel height was kept constant. Applying this extra condition, the applicable aspect ratio range reduces to 5 instead of 10 and moreover the optimum aspect ratio and Reynolds number becomes 2 and 1850 respectively. The irreversibility index has been proposed to magnify the effect of energy harvesting on optimum values derived from EGM technique. The irreversibility index indicates that without energy harvesting, the optimum values obtained from EGM method can only be interpreted as ideal values with a little industrial application. In other words, Results indicate that if an efficient thermodynamic machine is designed to harvest lost work, the best operating condition is one derived from EGM technique. The author suggestion is to combine thermoelectric devices with microscale heat sinks to harvest some portion of lost work and run the pump with less external power source.

References:

- [1] D.B. Tuckerman, R.F.W. Pease, "High-performance heat sinking for VLSI", *IEEE Electron Device Letters*, 2(5), 126-129, 1981.
- [2] W. Urbanek, J.N. Zemel, H. Bau, "An investigation of the temperature dependence of Poiseuille numbers in micro-channel flow", *Journal of Micromechanics and Microengineering*, 3, 206-208, 1993.
- [3] G.M. Mala, D. Li, J.D. Dale, "Heat transfer and fluid flow in microchannels", *International Journal of Heat and Mass Transfer*, 40, 3079-3088, 1997.
- [4] J. Pfahler, J. Harley, H. Bau, J.N. Zemel, "Gas and liquid flow in small channels", *Micromechanical Sensors, Actuators, and Systems*, 32, 49-58, 1991.
- [5] M.S El-Genk, M. Pourghasemi, "Analytical and Numerical Investigations of Friction Number for Laminar Flow in Microchannels", *Journal of Fluids Engineering*, 141 (3), 031102-1-031102-15.
- [6] J. Judy, D. Maynes, B.W. Webb, "Characterization of frictional pressure drop for liquid flows through microchannels", *International Journal of Heat and Mass Transfer*, 5, 3477-3489, 2002.

- [7] P.S. Lee, S.V. Garimella, "Thermally developing flow and heat transfer in rectangular microchannels of different aspect ratios", *International Journal of Heat and Mass Transfer*, 49, 3060–3067, 2006.
- [8] W. Qu, I. Mudawar, "Experimental and numerical study of pressure drop and heat transfer in a singlephase microchannel heat sink", *International Journal of Heat and Mass Transfer*, 45, 2549–2565, 2002.
- [9] M. Razi , M. Pourghasemi, "Direct Numerical Simulation of deformable droplets motion with uncertain physical properties in macro and micro channels". *Computer & Fluids*, 154 (1), 200-210, 2017.
- [10] S. J. Kim, "Methods for thermal optimization of microchannel heat sinks," *Heat Transfer Engineering*, 25 (1), 37–49, 2004.
- [11] S. V. Garimella and V. Singhal, "Single-phase flow and heat transport and pumping considerations in microchannel heat sinks", *Heat Transfer Engineering*, 25 (1), 15–25, 2004.
- [12] S. P. Jang and S. J. Kim, "Fluid flow and thermal characteristics of a mi-crochannel heat sink subject to an impinging air jet", *Journal of Heat Transfer*, 127 (7), 770–779, 2005.
- [13] J. Cruz, I. Amaya, R. Correa, "Optimal rectangular microchannel design, using simulated annealing, unified particle swarm and spiral algorithms, in the presence of spreading resistance", *Applied Thermal Engineering*, 84, 126-137, 2015.
- [14] G. Ibanez, A. Lopez, J. Pantoja, J. Moreira, J. A. Reyes, "Optimum slip flow based on the minimization of entropy generation in parallel plate microchannels", *Energy*, 50, 143-149, 2013.
- [15] M.S El-Genk, M. Pourghasemi, "Nusselt number and development length correlations for laminar flows of water and air in microchannels", *International Journal of Heat and Mass Transfer*, 133, 277-294, 2019.
- [16] R.K. Shah, A.L. London, *Laminar Flow Forced Convection in Ducts*, Academic Press, New York, 1978.
- [17] B. Kim, "An experimental study on fully developed laminar flow and heat transfer in rectangular microchannels", *International Journal of Heat and Mass Transfer*, 46, Part B, 224-232, 2016.